# Exceptionally directional sources with photonic-bandgap crystals

**R. Biswas**

*Department of Physics and Astronomy, Ames Laboratory and Microelectronics Research Center, Iowa State University, Ames, Iowa 50011*

**E. Ozbay, B. Temelkuran, and Mehmet Bayindir**

*Department of Physics, Bilkent University, Bilkent, Ankara 06533, Turkey*

**M. M. Sigalas**

*Department of Physics and Astronomy, Ames Laboratory and Microelectronics Research Center, Iowa State University, Ames, Iowa 50011 and Agilent Technologies, Inc., 3500 Deer Creek Road, Palo Alto, California 94306*

**K.-M. Ho**

*Department of Physics and Astronomy, Ames Laboratory and Microelectronics Research Center, Iowa State University, Ames, Iowa 50011*

Received January 3, 2001; revised manuscript received March 30, 2001

Three-dimensional photonic-bandgap crystals are used to design and fabricate uniquely directional sources and receivers. By utilizing the resonances of a Fabry–Perot cavity formed with photonic-bandgap crystals, we were able to create exceptionally directional sources by placing the sources within such a cavity. Very good agreement between finite-difference time-domain calculations and the experiment is obtained. Radiation patterns with half-power beam widths of less than 12 degrees were obtained. © 2001 Optical Society of America

*OCIS codes:* 270.1670, 050.2230, 230.5750, 260.2110.

## 1. INTRODUCTION

Photonic-bandgap materials are in one of the fastest growing subfields in optical physics. Photonic-bandgap (PBG) crystals have immense promise for manipulating and engineering the local photonic densities of states (DOS) and realizing novel electromagnetic phenomena.[1,2] By enhancing or suppressing the local photonic DOS, spontaneous emission can be tailored, creating novel phenomena in optical physics.

We describe here a powerful and elegant way for the modification of the photonic DOS by creating resonant cavities with photonic crystals and utilizing these to tailor the emission of sources. Our work has an analogy with past research in optical physics, where the modification of the local photonic DOS near atoms was studied. Atoms located near the walls experience a modified local photonic DOS that can change spontaneous emission. Purcell[3] was the first to recognize that spontaneous emission can be modified by the environment, especially by a cavity. A very powerful illustration of this effect is a Fabry–Perot type of cavity of linear dimension $L$ (Fig. 1). Such a cavity with perfectly reflecting walls only allows modes with wavelengths $\lambda_m = 2L/m$ or frequencies $\nu_m = mc_0/2L$. Both measurements and simulations found strongly modified directional emission patterns of atoms placed inside microcavities when the cavity frequencies were matched to the frequency of atomic emission.[4–6]

Photonic-bandgap crystals offer a completely novel method for engineering the emission of sources. A Fabry–Perot cavity can be created by simply separating the unit cells in a photonic-bandgap crystal by a displacement $d$, which is equivalent to generating a planar defect. The cavity modes are equivalent to the modes of a planar defect.[7] By adjusting the cavity separation, the defect frequency (such as for the fundamental mode, $m = 1$) can be tuned to lie within the photonic bandgap. As shown in Fig. 2 we displayed the measured frequencies as a function of the separation, $d$, of a Fabry–Perot cavity built around a three-dimensional (3-D) photonic crystal.[7] Then radiation can emerge from the cavity only at frequency $\nu_1$, with all other frequencies in the bandgap suppressed. The emission pattern of a source within the cavity is expected to be a narrow directional pattern.

## 2. COMPUTATIONAL METHOD

We study both theoretically and experimentally such photonic-crystal cavities using the layer-by-layer photonic crystal composed of dielectric rods that has a full robust 3-D photonic bandgap.[8] The dimensions can be scaled to generate any frequency range of interest. Since dielectric materials (such as silicon or alumina) have a broad wavelength range in the infrared, where absorption is negligible,[9] Maxwell's equations can be rescaled to a

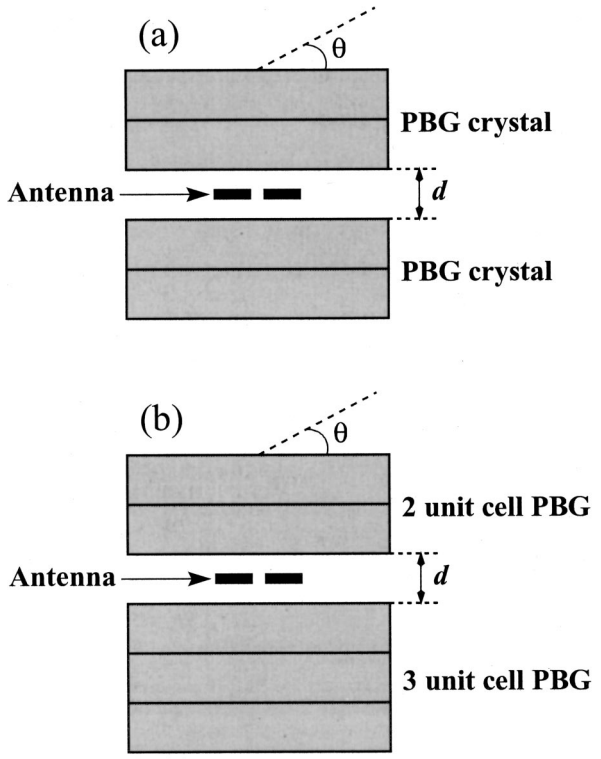


Fig. 1. Schematics of the cavity structures: (a) Symmetric Fabry–Perot cavity formed by photonic crystals composed of dielectric layers; (b) Asymmetric cavity formed by a three-unit cell PBG crystal separated from a two-unit cell PBG crystal.

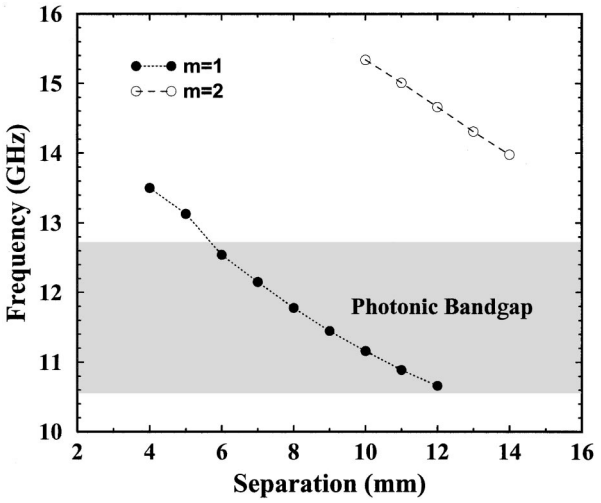


Fig. 2. Measured frequency of the planar defect mode of a Fabry–Perot cavity as a function of the cavity separation $d$. The photonic stop band extends from 10.6 to 12.7 GHz (gray region).

desired-length scale. This leads to a dielectric PBG crystal whose dimensions can be scaled to generate a bandgap at the desired wavelength range. For near-IR frequencies the photonic crystal has been fabricated by advanced silicon-processing techniques with rods of thicknesses of 0.18 $\mu$m and a rod-to-rod separation of 0.65 $\mu$m, generating a bandgap between 1.3 and 1.7 $\mu$m or centered at 1.5 $\mu$m,[10] which is ideally suited for optical communication applications. The structure has an attenuation of ~12 dB/unit cell. Alternatively, for the microwave regime, the rod thickness is 0.3 cm, with a rod-to-rod spacing of 1.1 cm generating a bandgap between 10.6 GHz and 12.7 GHz.[8]

We utilize the 3-D finite-difference time-domain (FDTD) technique to simulate the cavity emission. A dipole source is placed inside a cavity. The time-dependent Maxwell curl equations are numerically integrated to determine the radiation fields. The standard near-to-far field transformation[11] is used to determine the far-field radiation patterns. In this near-to-far field transformation, the electric and the magnetic equivalent currents are calculated at the surface of the parallelepiped that encloses the photonic crystal. The currents are calculated at specified frequencies from the tangential **H** and **E** fields by use of discrete Fourier transforms. These equivalent currents are integrated with the free-space Green's function to obtain the far zone **E** and **H** fields.[11]

Due to symmetry we only need to simulate one-fourth of the unit cell. The simulation space was divided into a mesh of 240 points × 240 points × 226 points for the asymmetric cavity and 240 points × 240 points × 194 points for the symmetric cavity. This corresponds to 20 grid spaces separating the center-to-center distance of the rods in each layer and 8 mesh points in the $z$ direction dividing the cross section of each rod. This mesh size provided good stability in the simulations and compared well with experiment in a previous work.[12] At the boundary of the simulation cell we use the second-order Liao absorbing boundary conditions.[13] Each layer of our PBG crystal is composed of 15 rods in each plane. We use rods ($n$ = 3.1) of square cross section. Past results[12] have showed that FDTD simulation compared very well with experimental measurements for dipole antennas placed on the surface of these 3-D PBG crystals. Typical computational runs for radiation patterns involved 2400 FDTD simulation steps with a continuous-wave excitation of the dipole source at a specified frequency. This required ~10 h of processor time on a Silicon Graphics Power Onyx with a RISC-10000 195-GHz processor and 1.5 GBytes of memory, running in serial mode.

## 3. DIRECTIONAL SOURCES AND DETECTORS

We first simulated a symmetric-cavity geometry where the walls were formed by two-unit cells (8 layers) of PBG on each side of the cavity (Fig. 1). We quote results for both the optical cavity and the microwave cavity. The cavity width, or the separation of the two sides of the cavity, is 20 grid spaces in the computational cell, and is equivalent to 48 nm for the optical cavity and 0.8 mm for the microwave cavity. We find that this cavity separation generates a primary defect mode near 1.5 $\mu$m or 12 GHz near the center of the bandgap for these cavities.

Using the FDTD technique we simulated a dipole oscillator source at the center of the cavity. An oscillating voltage of desired frequency is maintained across the dipole leads. The far-field radiation pattern of this dipole antenna is simulated at various frequencies. At the resonant frequency (1.55 $\mu$m/11.6 GHz) we found the radiation pattern to consist of two narrow cones in the forward and backward directions through the cavity walls (Fig. 3).

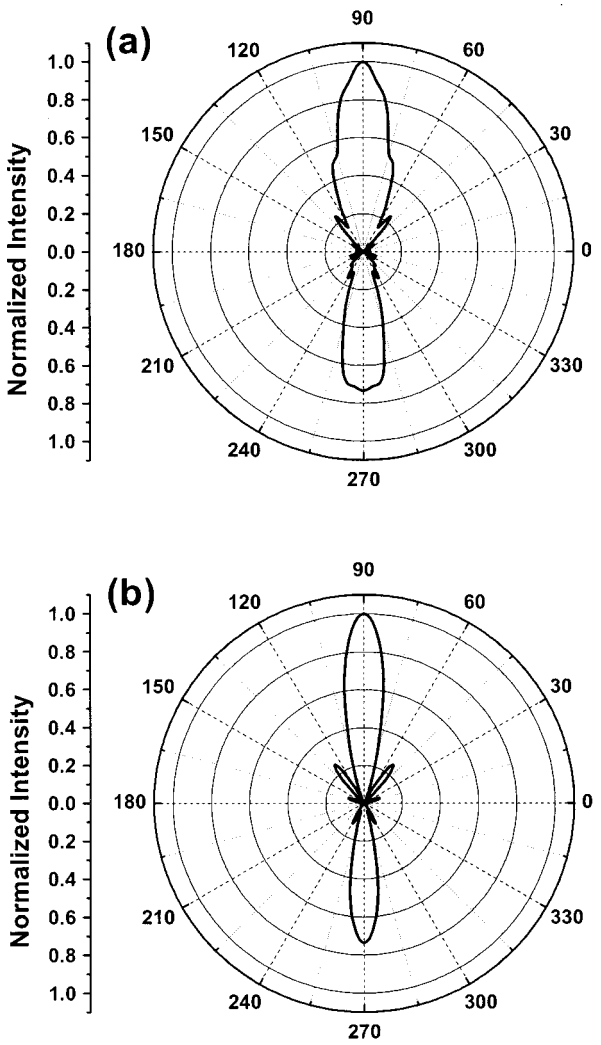


Fig. 3. Calculated radiation pattern for (a) $E$ plane and (b) $H$ plane from a dipole source at the center of a symmetric cavity, formed with two-unit cells of PBG crystal as the cavity wall. The dipole is driven at the resonant frequency of the cavity (which is 11.6 GHz for the microwave-scale PBG).

The radiation pattern has narrow half-widths of 16° in the $E$ plane and 11° in the $H$ plane. Such directional patterns would not be possible with a single dipole oscillator source. Such directionality can usually be achieved only with an antenna array. Because of time-reversal symmetry of the electromagnetic fields, this pattern also represents the pattern of a receiver.

The radiation pattern is highly directional because the radiation can only emerge from the cavity at the frequency of the defect mode. The radiation is suppressed at angles away from the normal, and the Fabry–Perot defect mode cannot be observed at large angles of incidence. At frequencies within the band edges, broad radiation patterns are observed.

The next step to enhance this resonant effect is to make the cavity asymmetric by having three-unit cells at the back of the cavity and retaining the two-unit cells on the front side. Although there is radiation emerging from both sides of the cell, there is an extra attenuation of 12 dB in the photonic crystal for the beam that emerges through the three-unit cell wall. This extra attenuation for the additional unit cell is typical for PBG frequencies[5,6] and effectively suppresses the backward lobe and generates a single radiation lobe in the forward direction. The dependence of the frequency of the defect mode on the asymmetric-cavity separation $d$ is very similar to the result in the symmetric cavity (Fig. 2). To optimize the pattern further, we chose a dipole of length $l=1.25\lambda$. For the free-dipole oscillator, this longer dipole provides a much narrower radiation pattern than the short half-wave free dipole, and the source pattern is shown in Ref. 14.

We obtain a single pencillike radiation pattern through the front side of the cavity (Fig. 4) with an exceedingly narrow full width at half-maxima of 14° in the $E$ plane and 12° in the $H$ plane. This uniquely directional pattern has only very weak sidelobes at ~30° to the normal and a radiation in the backside that is weaker by a factor of 10. The directionality was slightly improved by positioning the source away from the center of the cavity and toward the three-unit cell cavity wall. Because of the time-reversal symmetry this also represents the directional response of a detector placed inside the cavity. Di-

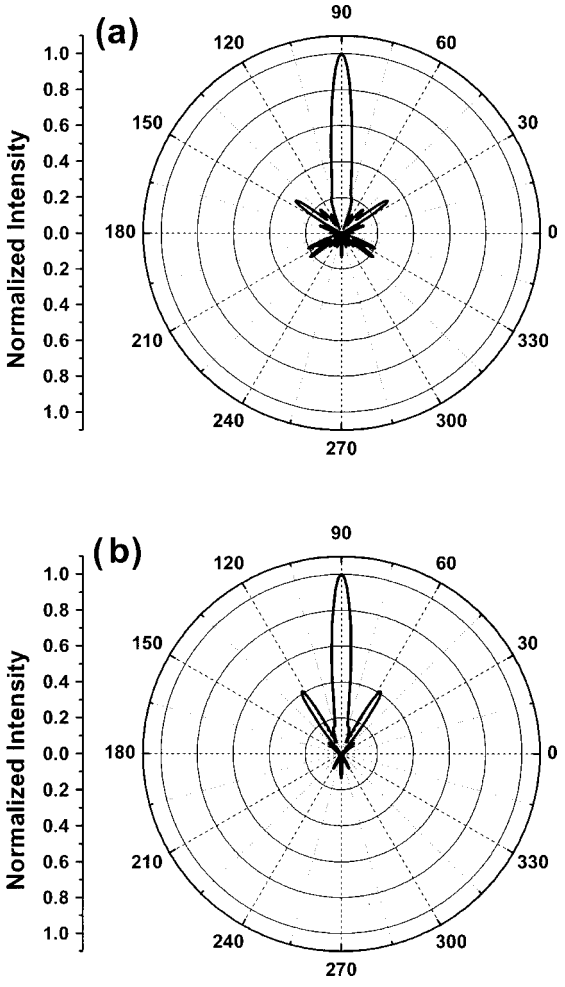


Fig. 4. Radiation pattern in (a) the $E$ plane and (b) the $H$ plane for a dipole source placed inside an asymmetric cavity formed by creating a cavity between a two-unit cell PBG and three-unit cell PBG crystal. All the radiation emerges in a narrow cone through the thinner two-unit cell crystal.

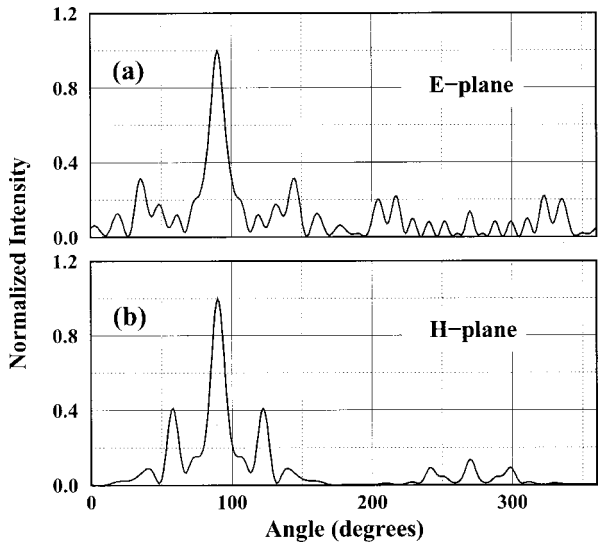


Fig. 5. Radiation pattern in (a) the $E$ plane and (b) the $H$ plane plotted in the linear scale, for the dipole source inside the asymmetric cavity. The forward direction covers the angles from 0 to 180°, whereas the backward direction through the three-unit cell PBG crystal is from 180° to 360°.

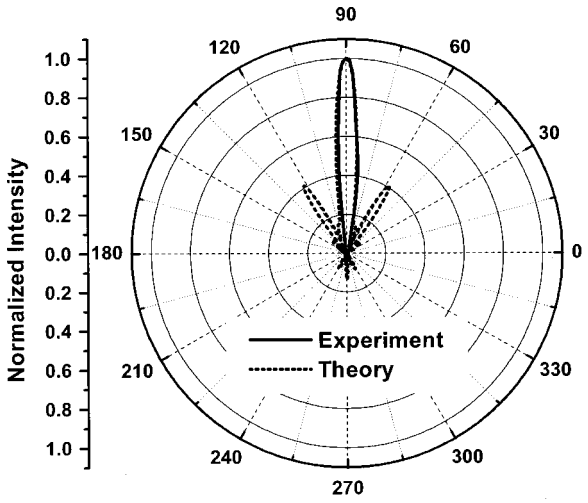


Fig. 6. Measured antenna radiation pattern from a monopole antenna placed inside the asymmetric cavity of Fig. 1, along with the comparison obtained by calculation.

rectional receivers can detect signals from a very narrow field of view, which is a desirable feature for detectors in astronomy applications. The half-widths of the radiation patterns are more clearly evident in the linear plot of the radiated intensity as a function of the polar angle (Fig. 5).

When the frequency of the source is increased above the resonant frequency the pattern develops sidelobes, although the central feature remains narrow and similar. At frequencies below resonance, the radiation pattern broadens. Our simulations predict a frequency window of ~ 2% around the resonant frequency for this unique directionality.

Extensive experimental measurements[15] have been performed on a cavity created from two and three-unit cells of a PBG crystal and a monopole antenna source. The experiment was facilitated by a PBG crystal operating at microwave frequencies. For this geometry a resonant frequency of $\nu_0 = 11.72$ GHz was found, and the measured antenna radiation (Fig. 6) displays a half-power full width of 12° in the $E$ plane and 11° in the $H$ plane.[15] In accordance with conventions[14] the $E$ plane contains the dipole, whereas the $H$ plane is perpendicular to the dipole. The theoretical calculations are in very good agreement with these measurements.

The power detected by a receiver placed in this resonant cavity was also measured as a function of frequency. At the resonance frequency a power enhancement of 180 (22.6 dB) was measured. The $Q$ factor, defined as the center frequency divided by the full width at half-maximum, was measured to be 895. For antennas with one major lobe the directivity is approximately given by

$$D = \frac{4\pi}{\Omega} = \frac{4\pi}{\Theta_1\Theta_2}, \tag{1}$$

where the beam solid angle $\Omega$ is given by the product of the half-power beam widths $\Theta_1$ and $\Theta_2$ in the two perpendicular $E$ and $H$ planes.[14] The measured (and computed) directivity from the half-power beam widths reaches a peak value of ~310. This is a major improvement over the configuration where the dipole antenna was placed on the photonic crystal surface, which had a directivity of ~10 and a directive gain of 8 (see Refs. 12, 16, and 17).

It is relevant to compare our resonant photonic-crystal antenna to traditional phased antenna arrays. A linear end-fire antenna array, where the phase difference between neighboring antennas is tuned to be $\beta = -kd$ ($d$ = separation, $k$ is the wave vector), can generate a primary narrow radiation lobe along the antenna axis.[14] A quarter-wave antenna separation ($d/\lambda = 0.25$) is frequently used. The beam width of this primary lobe decreases only slowly with the number of antennas in the array.[14] However, to produce narrow half-power beam widths of 12° similar to the present results (Fig. 4), one requires as many as ~320 antennas in the linear array, which is a formidable task for traditional antenna design. We note that a double-lobe radiation pattern with a half-width of 11° similar to Fig. 3 can alternatively be achieved with a traditional broadside antenna array with ~18 elements.

This photonic-crystal based resonant antenna is a uniquely directional source or receiver that offers very high gain in a narrow bandwidth of frequencies. We plot the maximum calculated intensity of the radiation lobe as a function of frequency (Fig. 7) to estimate the bandwidth of the antenna. The calculated bandwidth (Fig. 7) of this antenna (0.02–0.025 $\nu_0$) is equivalent to 0.3–0.4 GHz for the microwave crystal and is considerably broader than the experimentally determined value. The small frequency resolution (0.02 $\nu_0$) resulting from the finite time of the simulations may account for this difference.

## 4. COMPARISON OF THREE DIMENSIONS WITH ONE DIMENSION

Recently a one-dimensional (1-D) multilayer dielectric structure that has a single sharp defect mode has been fabricated by Thevenot *et al.*[18] The system was driven

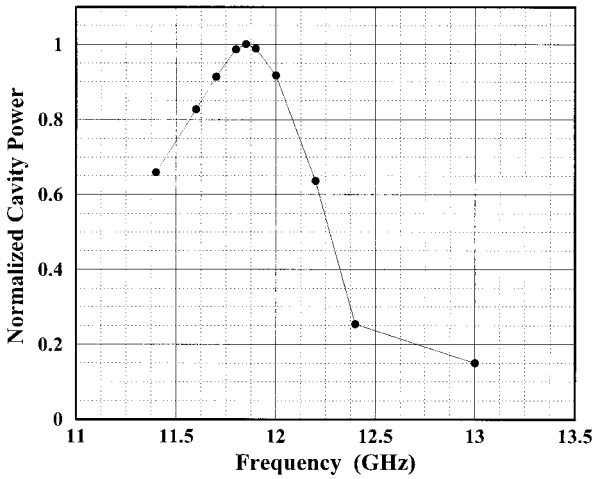


Fig. 7. Calculated output power of the dipole inside the asymmetric cavity as a function of the frequency. The dipole power is normalized to its maximum value.

by a patch antenna on a metal plate. The metal ground plane generated the image of the upper dielectric layers, so that only one-half of the structure was necessary for fabrication. At the resonant frequency of their 1-D cavity they found a directive radiation pattern with the directivity increasing from 8 dB to 19 dB.

The simpler 1-D structures do have an experimental advantage of easier fabrication over 3-D structures. However, we do find the performance of 3-D crystals to be superior to their 1-D counterparts. We have simulated 1-D cavities composed of dielectric layers ($n = 3.1$) separated by air. We have also simulated a cavity between these 1-D layers and have placed a dipole source within the cavity. Although we observed a narrowing of the radiation pattern, the directionality of the antenna radiation pattern is much inferior to that of the 3-D crystal cavity.

## 5. DISCUSSION

The early application of photonic crystals to the field of antennas and emission was to use the photonic crystals as a perfect reflector at frequencies within the bandgap and to place sources on the surface of the photonic crystal. When such antennas were driven at frequencies within the bandgap all the power was radiated in the air side with no power emerging from the PBG side.[12,16,19] This substantially reduced the large power loss of antennas on semiconductor substrates, where most of the power (>90%) can be lost as substrate modes.

However, the antennas on PBG substrates had radiation patterns that were sensitive to the height and lateral position of the antenna. This is because the antenna power depends on the local electric field at the substrate, which is a sharply varying function of the lateral position and height of the antenna on the substrate.[12,19] The radiation patterns of the present resonant antenna are far superior to those achieved with antennas on the PBG crystals. We also find resonant antennas are less sensitive to position within the cavity. However, the bandwidth of resonant antennas is less than for the antennas on PBG substrates.

Some preliminary experiments with atoms in optical cavities have already shown a narrowing of the emission pattern at the resonant frequency. Optical measurements have been taken that find sidelobes and a broadening of the emission pattern away from resonance, in good agreement with our simulations.

The resonant cavities offer a practical way to test predictions expected in optical physics, with the antenna being the analog of an emitting atom with cavity dimensions on the nanoscale, which can lead to a fundamental understanding of cavity electrodynamics. We anticipate that uniquely directional high-gain sources and detectors can be generated with this method.

## ACKNOWLEDGMENTS

We thank Gary Tuttle and Costas Soukoulis for many helpful suggestions and discussions. Ames Laboratory is operated by the U.S. Department of Energy and by Iowa State University under contract W-7405-Eng-82. We also acknowledge support by the Department of Commerce through the Center of Advanced Technology Development at Iowa State University.

E-mail address for R. Biswas is biswasr@ameslab.gov.

## REFERENCES

1. For a recent review, see articles in *Photonic Band Gap Materials*, C. M. Soukoulis, ed. (Kluwer, Dordrecht, The Netherlands, 1996).
2. J. D. Joannopoulos, R. D. Meade, and J. N. Winn, *Photonic Crystals: Molding the Flow of Light* (Princeton University Press, Princeton, N.J., 1995).
3. E. M. Purcell, "Modification of spontaneous emission," Phys. Rev. **69**, 681 (1946).
4. H. Yokohama and K. Ujihara, eds., *Spontaneous Emission and Laser Oscillation in Microcavities* (CRC Press, Boca Raton, Fla., 1995).
5. H. Yokohama, "Spontaneous and stimulated emission in the microcavity laser," in *Spontaneous Emission and Laser Oscillation in Microcavities*, H. Yokohama and K. Ujihara, eds. (CRC Press, Boca Raton, Fla., 1995), pp. 275–310.
6. G. Bjork and Y. Yamamota, "Spontaneous emission in dielectric planar microcavities," in *Spontaneous Emission and Laser Oscillation in Microcavities*, H. Yokohama and K. Ujihara, eds. (CRC Press, Boca Raton, Fla., 1995), pp. 189–236.
7. E. Ozbay and B. Temelkuran, "Reflection properties and defect formation in photonic crystals," Appl. Phys. Lett. **69**, 743–745 (1996).
8. E. Ozbay, A. Abeyta, G. Tuttle, M. Tringides, R. Biswas, C. T. Chan, C. M. Soukoulis, and K.-M. Ho, "Measurement of a three-dimensional photonic band gap in a crystal structure made of dielectric rods," Phys. Rev. B **50**, 1945–1948 (1994).
9. E. D. Palik, ed., *Handbook of Optical Constants of Solids* (Academic, Boston, 1991).
10. S. Lin and P. Fleming, "Three-dimensional photonic crystal with a stop band from 1.35 to 1.95 $\mu$m," Opt. Lett. **24**, 49–52 (1999).
11. A. Tavlove, *Computational Electromagnetics: The Finite-Difference Time-Domain Method* (Artech House, Boston, 1995).
12. M. M. Sigalas, R. Biswas, Q. Li, D. Crouch, W. Leung, R. Jacobs-Woodbury, B. Lough, S. Nielsen, S. McCalmont, G. Tuttle, and K.-M. Ho, "Dipole antennas on photonic band gap crystals: experiment and simulation," Microwave Opt. Technol. Lett. **15**, 153–158 (1997).
13. Z. P. Liao, H. L. Wong, B. P. Yang, and Y. F. Yuan, "A trans-

mitting boundary for transient wave analysis," Sci. China A, **27**, 1063–1076 (1984).
14. C. A. Balanis, *Antenna Theory: Analysis and Design* (Harper & Row, New York, 1982).
15. B. Temelkuran, M. Bayindir, E. Ozbay, R. Biswas, M. Sigalas, G. Tuttle, and K.-M. Ho, "Photonic crystal based resonant antenna with a very high directivity," J. Appl. Phys. **87**, 603–605 (2000).
16. E. R. Brown and O. B. McMahon, "High zenithal directivity from a dipole antenna on a photonic crystal," Appl. Phys. Lett. **68**, 1300–1302 (1994).
17. E. R. Brown, C. D. Parker, and E. J. Yablonovitch, "Radiation properties of a planar antenna on a photonic crystal substrate," J. Opt. Soc. Am. B **10**, 404–407 (1993).
18. M. Thevenot, C. Cheype, A. Reineix, and B. Jecko, "Directive photonic band gap antennas," IEEE Trans. Antennas Propag. **47**, 2115–2122 (1999).
19. M. P. Kesler, J. G. Maloney, B. L. Shirley, and G. S. Smith, "Antenna design with the use of photonic band gap materials as all dielectric planar reflectors," Microwave Opt. Technol. Lett. **11**, 169–174 (1996).